

Mechanical Properties of Powder Metallurgy (Ti-6Al-4V) with Hot Isostatic Pressing

Mohamed Abdulla Elfghi
Mechanical Engineering Department
Karabuk University
Karabuk, Turkey
elfghi@yahoo.co.uk

Mustafa Gunay
Mechanical Engineering Department
Karabuk University
Karabuk, Turkey
mgunay@karabuk.edu.tr

Abstract—Titanium alloys are widely used due to their high performance and low density in comparison with iron-based alloys. Their applications extend to aerospace and military in order to utilize their high resistance for corrosion. Understanding the mechanical properties and microstructure of titanium alloys is critical for performance optimization, as well as their implications on strength, plasticity, and fatigue. Ti-6Al-4V is an $\alpha+\beta$ two-phase alloy and is considered one of the most commonly used titanium alloys for weight reduction and high-performance. To avoid manufacturing defects, such as porosity and composition segregation, Hot Isostatic Pressing (HIP) is used to consolidate alloy powder. The HIP method is also used to facilitate the manufacturing of complex structures that cannot be made with forging and casting. In the current research, Ti-6Al-4V alloys were manufactured with HIP and the impact on heat treatment under different temperatures and sintering durations on the performance and microstructure of the alloy was studied. The results show changes in mechanical properties and microstructure with the increase of temperature and duration.

Keywords—titanium alloy; Ti-6-4; hot isostatic pressing (HIP)

I. INTRODUCTION

The utilization of titanium for industrial purposes became popular during the last fifty years due to its competitive properties in comparison with traditionally used metals, such as iron, steel, etc. [1]. Titanium alloys are commonly used in aerospace and military applications due to their low density and high resistance to corrosion, high performance, and strength. Despite being expensive and hard to manufacture, these alloys became the engineering choice for experts due to their light weight and high performance under high temperatures [2]. The applications of titanium alloys are correlated to their mechanical properties. Therefore, it is important to understand the factors that affect these properties in order to optimize their performance. The mechanical properties of titanium alloys, such as creep, fatigue, plasticity, and strength, are highly affected by their microstructure [3]. The small size of α grains are correlated to the increase in ultimate tensile strength [4]. One of the most common titanium alloys is Grade 5 (Ti-6Al-4V or Ti-6-4), which is used extensively for engineering and industrial purposes. Due to its high mechanical performance and facilitation of weight reduction, applications of this alloy include marine equipment, automotive, and aerospace. Medical

and pharmaceutical applications can also be found for Ti-6Al-4V due to its exceptional biocompatibility [5]. However, the alloy has a difficult machinability because of its low thermal conductivity and high strength to density ratio [6]. Ti-6-4 is classified as an $\alpha+\beta$ two phase alloy with wide usage range in mechanical applications. Due to the structure complexity of the manufactured components and defects such as composition segregation and porosity, forging and casting is not the most preferred manufacturing method [7]. Thus, Hot Isostatic Pressing (HIP) is used for the consolidation of alloy powder in order to facilitate manufacturing complex components and avoid those defects [8]. The HIP method has also economic advantages as it maximizes the utilization of material and reduces cost [9]. In [10], further advantages were found for the HIP on Ti-6-4 on the microstructure level. Several studies attempted to optimize the heat and pressure conditions of the alloy in order to reach optimum performance. Some studies solely tested the heat or pressure change implications on titanium alloys, while a few investigated the change in both parameters [11]. Authors in [12] investigated the heat and pressure conditions of the HIP and the cooling rate of the Ti-6-4 samples on their microstructure and mechanical properties. They found that temperatures ranging between 900 and 940°C and a pressure of 100MPa yield the most optimized tensile strength, with sample holding for 3 hours in room temperature. Authors in [13] used HIP with high temperature and pressure conditions: 1200°C and 120MPa, while samples cooled in the furnace for 3 hours. Microstructure analysis showed an increase on the needle structures of Ti-6-4 and an increase in the nano hardness and the wear resistance of the samples. In the current study, Ti-6-4 alloys were manufactured under HIP and the samples were put under very high temperatures with different exposure timings. The impacts on wear resistance, microstructure, and mechanical properties were investigated and compared to the results of previous research for verification and possible enhancements on the properties of the alloy.

II. RESEARCH AIM AND METHODS

A. Research Aim

The aim of this research was to investigate the effect of very high heat exposure on Ti-6Al-4V alloys manufactured by HIP by comparing samples with different exposure durations.

Corresponding author: Mohamed Abdulla Elfghi

B. Material and Sample Preparation

The Ti-6-4 alloy used in the experiment was prepared through the cost-effective Blended Elemental (PM) technique. The hydrogenated titanium powder (3.5% H wt, Ti particle size 100 μ m) was mixed with 60Al-40V master alloy powder with particle size ranging between 40 to 63 μ m in order to obtain the required alloy composition [15], as shown in Table I.

TABLE I. CHEMICAL COMPOSITION OF THE ALLOY BY WT%

| Ti | Al | V | Fe | O | N | H |
|---------|------|------|-----|------|------|-------|
| Balance | 6.21 | 4.12 | 0.0 | 0.18 | 0.04 | 0.004 |

The powder was blended for 1200s (20m) and die pressed under 300MPa at a temperature of 500 $^{\circ}$ C for 4h to form green compacts of 60 \times 60 \times 3mm, as shown in Figure 1. The approximate density of the sintered alloy was determined through hydrostatic weighing as 4.42g/cm³, corresponding to 97.73% of its theoretical value. The compacted specimens are shown in Figure 2. For each produced sample, 50g of alloy powder was used, while the final average weight of each of the nine produced sample was 47.844g.



Fig. 1. Pressing and heating of the Ti-6-4 powder



Fig. 2. Specimens produced after pressing

The sintering of the specimens was performed in a vacuum furnace at a vacuum pressure of 10⁻³Pa. The nine specimens were divided into three groups as shown in Table 2. Three temperatures were applied: 1200 $^{\circ}$ C, 1300 $^{\circ}$ C and 1400 $^{\circ}$ C, at 2, 4 and 8h for each group. The described properties of powder metallurgy compacts are not comparable to the obtained wrought metal. It is expected that the sintered metal would have lower ductility, for both alloyed and unalloyed titanium, than the wrought metal [16].

TABLE II. SPECIMENS AND SINTERING CONDITIONS

| Group | Specimen | Furnace temperature ($^{\circ}$ C) | Sintering duration (h) |
|-------|----------|-------------------------------------|------------------------|
| A | A1 | 1200 | 2 |
| | A2 | | 4 |
| | A3 | | 8 |
| B | B1 | 1300 | 2 |
| | B2 | | 4 |
| | B3 | | 8 |
| C | C1 | 1400 | 2 |
| | C2 | | 4 |
| | C3 | | 8 |

Five tests were performed on each sample: wear resistance test, microhardness test, XRF analysis, XRD analysis, and SEM analysis. The results are presented and discussed along with the relevant literature below.

III. RESULTS AND DISCUSSION

A. Wear Resistance

The specimens were subjected to a wear resistance test, where machine parameters were set as shown in Table III.

TABLE III. WEAR RESISTANCE TEST PARAMETERS

| Parameter | Unit | Value |
|------------------|------|----------|
| Load | N | 20 |
| Stroke | mm | 7 |
| Test cycles | | 14285.71 |
| Sliding distance | m | 200 |
| Sliding speed | mm/s | 56 |
| Frequency | Hz | 4 |

As shown in Figure 3, the friction coefficient for specimens in group A differed with the sintering duration. While the maximum friction coefficient increased from 3.054 in A1 to 3.882 in A2, it decreased to 1.929 in A3, which corresponds to the longest sintering duration.

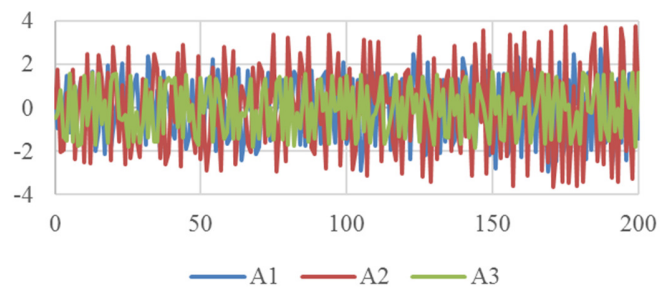


Fig. 3. Wear resistance friction coefficient change for Group A

In A1, fluctuations with an increase in friction appear between zero to 40m. Smooth sliding gaps started appearing afterwards with the maximum friction towards the end of the distance. Specimen A2 showed high fluctuation rate with a steady overall increase in friction, while A3 showed a steady friction coefficient with a wave of higher friction between 5 to 35m. The results for group B specimens are presented in Figure 4. A reduction in the overall friction coefficient was found in B2. Specimen B1 showed an increase of friction between 0 to 30m and had a maximum coefficient of 3.07. Specimens B2

and B3 showed more steady fluctuations at periodical intervals, with maximum coefficients of 2.109 and 3.382 respectively.

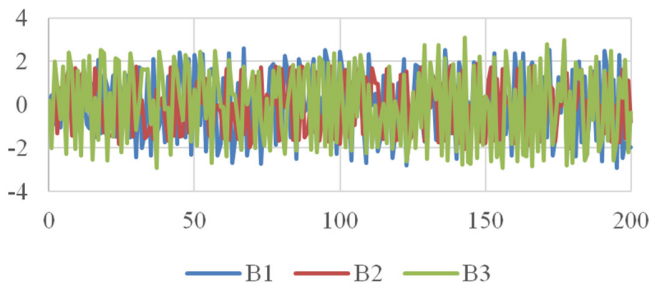


Fig. 4. Wear resistance friction coefficient change for Group B

B. Microhardness Test

Vickers microhardness test was conducted by applying a load of 1kg for 15s by a ball indicator. Values were measured through a calibrated optical microscope for the stress in MPa, as shown in Table IV.

TABLE IV. HARDNESS TEST VALUES

| Temperature(°C) | Time (h) | Value (1) | Value (2) | Value (3) | Average |
|-----------------|----------|-----------|-----------|-----------|---------|
| 1200 | 2 | 331 | 333 | 319 | 327 |
| 1200 | 4 | 389 | 398 | 405 | 397 |
| 1200 | 8 | 375 | 332 | 364 | 357 |
| 1300 | 2 | 403 | 387 | 379 | 389 |
| 1300 | 4 | 433 | 454 | 481 | 456 |
| 1300 | 8 | 488 | 491 | 499 | 485 |
| 1400 | 2 | 599 | 533 | 599 | 577 |
| 1400 | 4 | 427 | 481 | 477 | 461 |
| 1400 | 8 | 494 | 424 | 461 | 459 |

The average hardness values are presented in Figure 5. The hardness value of group A increased with the increase of sintering time between 2h and 4h, while it dropped at 8h. For

group B, the hardness value increased at both 2 and 4h, while it decreased for both sintering times for group C. Generally, microhardness values increased with the increase of heat treatment temperatures, while increased sintering times decreased hardness values. Authors in [17, 18] showed the increase in microhardness values between heat treated and untreated Ti-6-4 samples and authors in [19] reported a decrease in the hardness values with the increase of heat treatment temperatures without specifying changes in sintering durations.

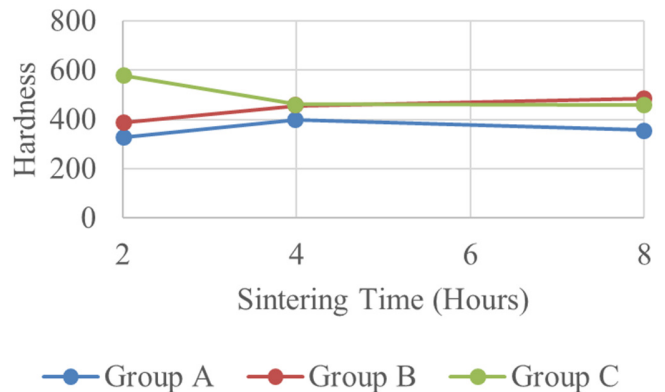


Fig. 5. Average hardness values for groups A, B and C

C. XRF Analysis

X-ray fluorescence (XRF) is a microscopy method used to determine the concentration of metals in an alloy in a specified area. The method is based on the interaction between the x-ray arrays with the matter through dislodging electrons from atoms and measuring the energy resulting to correlate it with a specific element [20]. Table V shows the results of the XRF analysis in the tested alloy.

TABLE V. XRF ANALYSIS OF THE ALLOY

| Component | Result | Unit | Det. limit | EL line | Intensity | w/o normal | Analyzing depth (mm) |
|-----------|---------|-------|------------|---------|-----------|------------|----------------------|
| B | 0.7751 | Mass% | 0.11345 | B-KA | 0.1816 | 0.9545 | |
| C | 3.1998 | Mass% | 0.03225 | C-KA | 4.4768 | 3.9402 | |
| N | 13.1932 | Mass% | 0.15751 | N-KA | 3.9806 | 16.2459 | |
| O | 30.8619 | Mass% | 1.09191 | O-KA | 0.4586 | 38.0030 | |
| Na | 0.0814 | Mass% | 0.01053 | Na-KA | 0.1706 | 0.1002 | 0.0030 |
| Mg | 0.0781 | Mass% | 0.00738 | Mg-KA | 0.5700 | 0.0962 | 0.0046 |
| Al | 0.4155 | Mass% | 0.00380 | Al-KA | 9.1576 | 0.5116 | 0.0069 |
| Si | 0.1610 | Mass% | 0.00156 | Si-KA | 3.7107 | 0.1982 | 0.0099 |
| P | 1.8753 | Mass% | 0.00281 | P-KA | 121.6887 | 2.3092 | 0.0137 |
| S | 0.1542 | Mass% | 0.00082 | S-KA | 8.6498 | 0.1899 | 0.0174 |
| Cl | 0.0401 | Mass% | 0.00255 | Cl-KA | 0.6165 | 0.0493 | 0.0240 |
| K | 0.0041 | Mass% | 0.00221 | K-KA | 0.1213 | 0.0051 | 0.0506 |
| Ca | 0.0198 | Mass% | 0.00266 | Ca-KA | 0.6777 | 0.0244 | 0.0658 |
| Ti | 47.7941 | Mass% | 0.02561 | Ti-KA | 432.8491 | 58.8530 | 0.1127 |
| V | 0.6622 | Mass% | 0.05760 | V-KA | 0.6306 | 0.8154 | 0.0402 |
| Fe | 0.6684 | Mass% | 0.00446 | Fe-KA | 13.8373 | 0.8230 | 0.0619 |
| Ni | 0.0041 | Mass% | 0.00247 | Ni-KA | 0.1708 | 0.0050 | 0.0919 |
| Cu | 0.0047 | Mass% | 0.00249 | Cu-KA | 0.2469 | 0.0057 | 0.1119 |
| Mo | 0.0071 | Mass% | 0.00126 | Mo-KA | 2.8908 | 0.0088 | 0.8550 |

The analysis depth ranged between 0.0030 to 0.8550mm. The titanium percentage reduced from 58.85% to 47.79%, while the percentages of Al and V reduced from 5.12% to

4.16% and from 8.15% to 6.62% respectively. The 90:6:4 ratio has been confirmed for the Ti-6-4 in various studies. Authors in [21] tested 4 samples of Ti-6-4 and confirmed the ratio with

error margins ranging between 0.13% and 10%, while authors in [22] identified 5.5% aluminium, 3.87% vanadium, and 0.22% iron by weight.

D. XRD Analysis

Identification of crystalline material in the samples that were subject to heat treatment was carried out through an X-Ray powder Diffraction (XRD) analysis. Figure 6 shows the peaks of 8 samples, which are identical in phase pattern and position, while differing in intensity. The higher the temperature and duration of the heat treatment, the higher is the intensity.

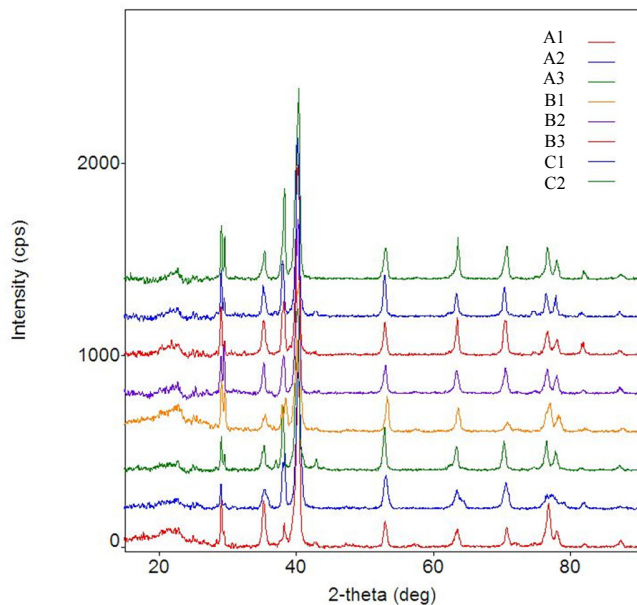


Fig. 6. Diffractogram of XRD analysis

The shift in the peaks with the increase of the heat treatment conditions is caused by the creation of equilibrium phases of the lamellar structure $\alpha+\beta$. The decrease in the width accompanied with the increase in intensity of the peaks is caused by the non-equilibrium α phase of the non-treated samples and the transformation to the equilibrium phase with heat treatment [23].

E. Scanning Electron Microscopy (SEM)

The specimens A1 to C2 were analyzed through scanning electron microscopy (Figures 7-14). The behavior of aluminum and vanadium vary under heat treatment. While Al tends to enter the α phase, the V tends to enter the β phase [24]. In the images taken for the 8 specimens at the same magnification, the dark regions show the α phase, while the light regions present the β phase [25]. The presence of delamination wear, abrasion and debris in the SEM pictures of Ti-6Al-4V is in accordance with the test results of other titanium alloy testing [26].

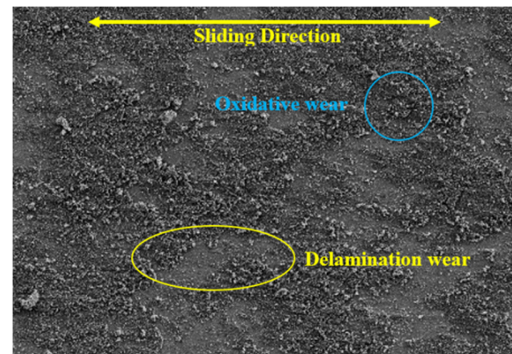


Fig. 7. SEM image of heat-treated specimens at $\times 500$ for A1 (layer thickness: A1=8.8 μm)

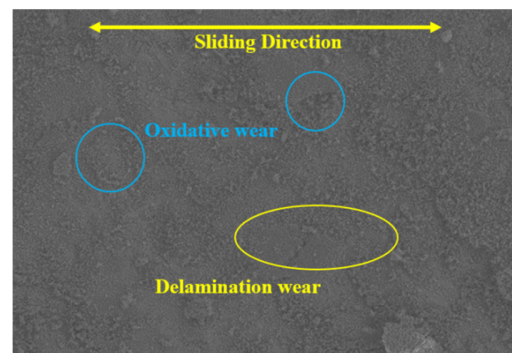


Fig. 8. SEM image of heat-treated specimens at $\times 500$ for A2 (layer thickness: A2=8.9 μm)

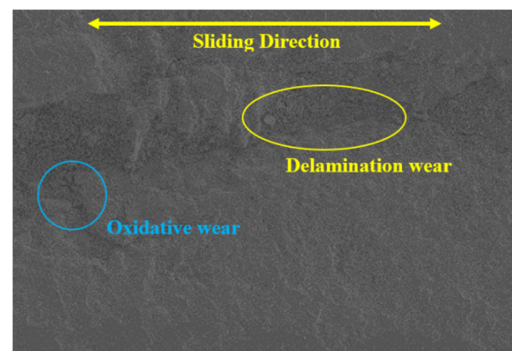


Fig. 9. SEM image of heat-treated specimens at $\times 500$ for A3 (layer thickness: A3=11.5 μm)

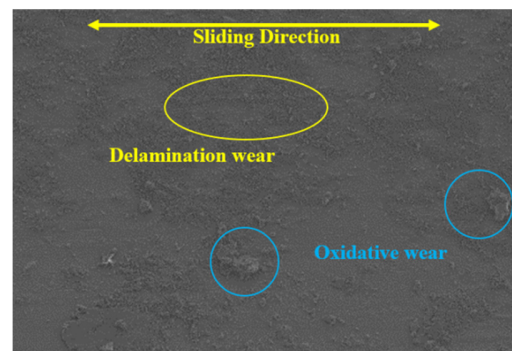


Fig. 10. SEM image of heat-treated specimens at $\times 500$ for B1 (layer thickness: B1=11.0 μm)



Fig. 11. SEM image of heat-treated specimens at $\times 500$ for B2 (layer thickness: B2=10.4 μm)

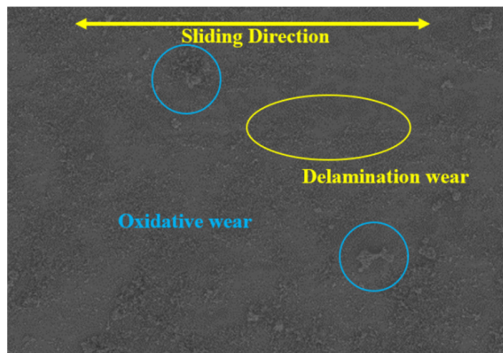


Fig. 12. SEM image of heat-treated specimens at $\times 500$ for B3 (layer thickness: B3=10.4 μm)

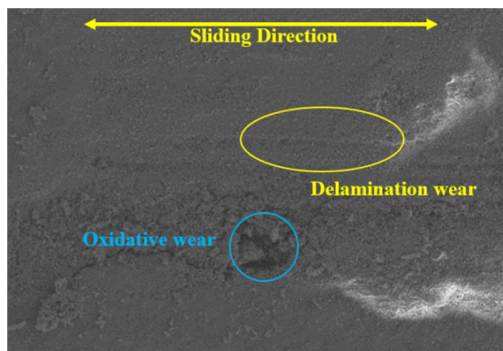


Fig. 13. SEM image of heat-treated specimens at $\times 500$ for C1 (layer thickness: C1=10.5 μm)

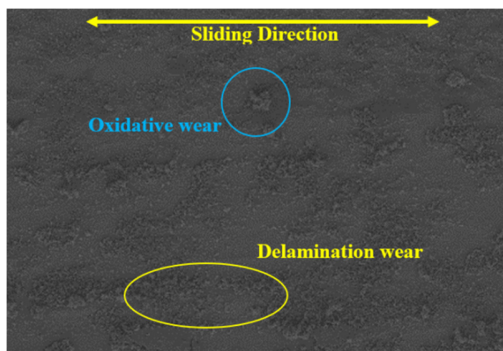


Fig. 14. SEM image of heat-treated specimens at $\times 500$ for C2 (layer thickness: C2=9.7 μm)

IV. CONCLUSION

In the current research, Ti-6Al-4V alloys were manufactured with the HIP method and the impact of heat treatment, under different temperatures and sintering durations on the performance and microstructure of the alloy, was studied. Three temperatures were tested (1200°C, 1300°C and 1400°C) with exposure durations of 2, 4 and 8 hours. The results show that sintering temperatures and durations had significant effects on wear resistance and hardness, namely higher temperatures and longer durations reduced wear resistance and hardness. XRD analysis showed a shift in the peaks with the increase of temperature and sintering duration, while an equilibrium in lamellar structure $\alpha+\beta$ was achieved. The peaks were increased in intensity and reduced in width. Moreover, SEM analysis showed that the α and β phases were balanced with the heat treatment.

REFERENCES

- [1] D. Aroussi, B. Aour, A. S. Bouaziz, "A comparative study of 316L stainless steel and a titanium alloy in an aggressive biological medium", *Engineering, Technology & Applied Science Research*, Vol. 9, No. 6, pp. 5093-5098, 2019
- [2] R. A. Antunes, C. A. F. Salvador, M. C. L. D. Oliveira, "Materials selection of optimized titanium alloys for aircraft applications", *Materials Research*, Vol. 21, No. 2, Article ID 20170979, 2018
- [3] G. Lutjering, "Property optimization through microstructural control in titanium and aluminum alloys", *Materials Science and Engineering: A*, Vol. 263, No. 2, pp. 117-126, 1999
- [4] G. Lutjering, "Influence of processing on microstructure and mechanical properties of ($\alpha+\beta$) titanium alloys", *Materials Science and Engineering: A*, Vol. 243, No. 1-2, pp. 32-45, 1998
- [5] C. N. Elias, J. H. C. Lima, R. Valiev, M. A. Meyers, "Biomedical applications of titanium and its alloys", *The Journal of the Minerals, Metals & Materials Society*, Vol. 60, pp. 46-49, 2008
- [6] S. A. Niknam, R. Khettabi, V. Songmene, "Machinability and machining of titanium alloys: A review", in: *Machining of Titanium Alloys*, Springer, 2014
- [7] G. Singh, I. Sen, K. Gopinath, U. Ramamurty, "Influence of minor addition of boron on tensile and fatigue properties of wrought Ti-6Al-4V alloy", *Materials Science and Engineering: A*, Vol. 540, pp. 142-151, 2012
- [8] R. P. Guo, L. Xu, J. F. Lei, R. Yang, "Effects of porosity and Re-HIP on properties of Ti-6Al-4V alloy from atomized powder", *Applied Mechanics and Materials*, Vol. 552, pp. 274-277, 2014
- [9] H. V. Atkinson, S. Davies, "Fundamental aspects of hot isostatic pressing: An overview", *Metallurgical and Materials Transactions A*, Vol. 31, No. 12, pp. 2981-3000, 2000
- [10] D. P. DeLo, H. R. Piehler, "Early stage consolidation mechanisms during hot isostatic pressing of Ti-6Al-4V powder compacts", *Acta Materialia*, Vol. 47, No. 9, pp. 2841-2852, 1999
- [11] K. Zhang, J. Mei, N. Wain, X. Wu, "Effect of hot-isostatic-pressing parameters on the microstructure and properties of powder Ti-6Al-4V hot-isostatically-pressed samples", *Metallurgical and Materials Transactions A*, Vol. 41, No. 4, pp. 1033-1045, 2010
- [12] L. Xu, R. Guo, C. Bai, J. Lei, R. Yang, "Effect of hot isostatic pressing conditions and cooling rate on microstructure and properties of Ti-6Al-4V alloy from atomized powder", *Journal of Materials Science & Technology*, Vol. 30, No. 12, pp. 1289-1295, 2014
- [13] C. Cai, B. Song, C. Qiu, L. Li, P. Xue, Q. Wei, J. Zhou, H. Nan, H. Chen, Y. Shi, "Hot isostatic pressing of in-situ TiB/Ti-6Al-4V composites with novel reinforcement architecture, enhanced hardness and elevated tribological properties", *Journal of Alloys and Compounds*, Vol. 710, pp. 364-374, 2017
- [14] O. M. Ivasishin, V. M. Anokhin, A. N. Demidik, D. G. Savvakina, "Cost-effective blended elemental powder metallurgy of titanium alloys for

- transportation application”, Key Engineering Materials, Vol. 188, pp. 55-62, 2000
- [15] M. Ahmed, A. A. Gazder, D. G. Savvakina, O. M. Ivasishin, E. V. Pereloma, “Microstructure evolution and alloying elements distribution between the phases in powder near- β titanium alloys during thermo-mechanical processing”, Journal of Materials Science, Vol. 47, pp. 7013-7025, 2012
- [16] M. Ustundag, R. Varol, “Comparison of impact properties of recycled and commercially available PM titanium alloys”, Journal of Engineering Sciences and Design, Vol. 7, No. 2, pp. 232-237, 2019
- [17] Y. C. Wang, T. G. Langdon, “Effect of heat treatment on microstructure and microhardness evolution in a Ti-6Al-4V alloy processed by high-pressure torsion”, Journal of Materials Science, Vol. 48, No. 13, pp. 4646-4652, 2013
- [18] A. O. Abdalla, A. Amrin, S. Muhammad, M. A. A. Hanim, “Effect of heat treatment parameters on the microstructure and microhardness of Ti-6Al-4V alloy”, AIP Conference Proceedings, Vol. 1865, No. 1, Article ID 030001, 2017
- [19] S. M. Ahmadi, R. K. A. K. Jain, A. A. Zadpoor, C. Ayas, V. A. Popovich, “Effects of heat treatment on microstructure and mechanical behaviour of additive manufactured porous Ti6Al4V”, IOP Conference Series: Materials Science and Engineering, Vol. 293, Article ID 012009, 2017
- [20] R. Zhang, L. Li, Y. Sultanbawa, Z. P. Xu, “X-ray fluorescence imaging of metals and metalloids in biological systems”, American Journal of Nuclear Medicine and Molecular Imaging, Vol. 8, No. 3, pp. 169-188, 2018
- [21] T. K. Hamad, H. T. Salloom, “Determination of species concentrations of Ti-6Al-4V titanium alloys using calibration free laser induced breakdown spectroscopy”, European Journal of Engineering Research and Science, Vol. 3, No. 8, pp. 50-55, 2018
- [22] K. A. Lee, Y. K. Kim, J. H. Yu, S. H. Park, M. C. Kim, “Effect of heat treatment on microstructure and impact toughness of Ti-6Al-4V manufactured by selective laser melting process”, Archives of Metallurgy and Materials, Vol. 62, No. 2B, pp. 1341-1346, 2017
- [23] B. Vrancken, L. Thijs, J. P. Kruth, J. V. Humbeeck, “Heat treatment of Ti6Al4V produced by selective laser melting: Microstructure and mechanical properties”, Journal of Alloys and Compounds, Vol. 541, pp. 177-185, 2012
- [24] R. Reda, A. H. Hussein, A. Nofak, E. S. M. E. Banna, “Optimizing the mechanical properties of Ti-6Al-4V castings”, International Journal of Mechanical and Production Engineering Research and Development, Vol. 5, No. 1, pp. 83-104, 2015
- [25] P. Aliprandi, F. Giudice, E. Guglielmino, A. Sili, “Tensile and creep properties improvement of Ti-6Al-4V alloy specimens produced by electron beam powder bed fusion additive manufacturing”, Metals, Vol. 9, No. 11, Article ID 1207, 2019
- [26] A. W. E. Morsy, “Wear analysis of a Ti-5Al-3V-2.5Fe alloy using a factorial design approach and fractal geometry”, Engineering, Technology & Applied Science Research, Vol. 8, No. 1, pp. 2379-2384, 2018